An Image Super-Resolution Algorithm for Different Error Levels Per Frame

Hu He and Lisimachos P. Kondi, *Member, IEEE*

***Abstract*—In this paper, we propose an image super-resolution (resolution enhancement) algorithm that takes into account inaccurate estimates of the registration parameters and the point spread function. These inaccurate estimates, along with the additive Gaussian noise in the low-resolution (LR) image sequence, result in different noise level for each frame. In the proposed algorithm, the LR frames are adaptively weighted according to their reliability and the regularization parameter is simultaneously estimated. A translational motion model is assumed. The convergence property of the proposed algorithm is analyzed in detail. Our experimental results using both real and synthetic data show the effectiveness of the proposed algorithm.**

***Index Terms*—Regularization, resolution enhancement, super-resolution.**

I. Introduction

THE objective of super-resolution, or resolution enhancement, is to reconstruct a high-resolution (HR) image from a sequence of low-resolution (LR) images. The LR sequence experiences different degradations from frame to frame, such as point spread function (PSF) blurring, motion, subsampling and additive noise. Each frame of the LR sequence only brings partial information of the original HR image. However, if there exists subpixel motion between these LR frames, each frame will bring unique partial information of the original HR image. Furthermore, if enough of such unique-information-bearing LR frames are available, digital image/video processing can be applied to recover the HR image.

The direct reverse solution from interpolation, motion compensation and inverse filtering is ill-posed due to the existence of additive noise, even in the cases where perfect motion registration is available and the PSF of the optical lens is known. Under these circumstances, the original HR image can not be "fully" recovered. Many approaches have been proposed to seek a stable solution with good visual quality to overcome the ill-posedness of the super-resolution. To our knowledge, the earliest effort was from Tsai and Huang [1]. Their method operates on the noise-free data in the frequency domain and capitalizes on the shifting property of the Fourier Transform and the aliasing relationship between the continuous Fourier transform (CFT) and the discrete Fourier transform (DFT). This technique was further improved by Tekalp *et al.* in [2] by taking into account a linear shift invariant (LSI) blur PSF and using a least squares approach to solving the system of equations. Kim *et al.* [3] also extended this technique for noisy data and derived a weighted least squares algorithm. However, these methods are applicable only to global motion that was known *a priori*. Most of the other resolution enhancement techniques that have appeared in the literature operate in the spatial domain. A projection onto convex sets (POCS) approach was formulated by Stark and Oskoui [4]. In this method, the space of HR images is intersected with a set of convex constraint sets representing desirable image characteristics, such as positivity, bounded energy, fidelity to data, smoothness, etc. The POCS approach has been extended to time-varying motion blur in [5], [6]. Block matching or phase correlation was applied to estimate the registration parameters in [5].

Another class of resolution enhancement algorithms is based on stochastic techniques. Methods in this class include maximum likelihood (ML) [7] and maximum *a posteriori* (MAP) approaches [8]–[11]. MAP estimation with an edge preserving Huber–Markov random field image prior is studied in [8]–[10]. MAP based resolution enhancement with simultaneous estimation of registration parameters (motion between frames) has been proposed in [11]–[15].

By using a specific Gaussian–Markov random field (GMRF) image prior with local clique, the MAP method is equivalent to the regularization approach. The cost function of MAP method is regularized with a regularization parameter. In most previous works on image restoration, a special case of resolution enhancement, regularization is widely used to avoid the ill-posed problem of inverse filtering [16], [17]. The regularization parameter of the cost function plays a very important role in the reconstruction of the HR image. The L-curve method was used to estimate this parameter in [18], where the desired "L-corner," the point with maximum curvature on the L-curve, was chosen as the one corresponding to the regularization parameter. Iterative adaptive algorithms with automatically updated regularization parameter have been proposed in [13] with much less computational cost and better visual quality.

The precise registration of the subpixel motion and knowledge of the PSF are very important to the reconstruction of the HR image. However, precise knowledge of these parameters is not always assured in real applications. Lee and Kang [19] proposed a regularized adaptive HR reconstruction considering inaccurate subpixel registration. Two methods for the estimation of the regularization parameter for each LR frame (channel) were advanced, based on the approximation that the registration error noise is modeled as Gaussian with standard deviation (STD) proportional to the degree of the registration error. The convergence of these two methods to the unique

Manuscript received June 23, 2002; revised February 14, 2005. The associate editor coordinating the review of this manuscript and approving it for publication was Dr. Tamas Sziranyi.

The authors are with the Department of Electrical Engineering, University at Buffalo, The State University of New York, Buffalo, NY 14260 USA (e-mail: huhe@eng.buffalo.edu; lkondi@eng.buffalo.edu).

Digital Object Identifier 10.1109/TIP.2005.860599

1057-7149/04$20.00 © 2006 IEEE

Authorized licensed use limited to: University of Ioannina. Downloaded on November 19, 2009 at 08:29 from IEEE Xplore. Restrictions apply.

global solution was observed experimentally using different initial conditions for the HR image. However, the convergence of these methods was not rigorously proved. Image restoration from partially known blurs was studied in the hierarchical Bayesian framework in [20]. The unknown component of the PSF was modeled as stationary zero-mean white noise. Two iterative algorithms were proposed using evidence analysis (EA), which in effect are identical to the regularized constrained total least squares filter and linear minimum mean square-error filter, respectively.

Robust super-resolution techniques have appeared in [21]–[23] and take into account the existence of outliers (data that do not fit the model very well). In [21], a median filter is used in the iterative procedure to obtain the HR image. The robustness of this method is good when the errors from outliers are symmetrically distributed, which are proved to be, after a biased detection procedure. However, a threshold is needed to decide whether the bias is due to outlier or aliasing information. Also, the mathematical justification of this method is not analyzed. In [22] and [23], a robust super-resolution method was proposed based on the use of the L_1 norm in both the regularization and the measurement term of the penalty function. Robust regularization based on a bilateral prior was proposed to deal with different data and noise models. Also, the mathematical justification of a "shift and add" was provided and related to L_1 norm minimization when relative motion is pure translational, and the PSF and decimation factor are common and space invariant in all LR images.

The technique in [11]–[15] was later extended to the cases in which the LR frames are contaminated by additive white Gaussian noise (AWGN) with different variance for each frame [24]. The motivation is that when AWGN with different variance is the only noise source added to the LR images, the residual term of the cost function should be weighted by the inverse of the variance to each frame (channel). Furthermore, when there exist other types of noise (errors) in the reconstruction process during resolution enhancement, some form of weighting should also be given to each channel to reduce the error effect. Therefore, in this paper, we take all three types of noise (blur noise due to inaccurate estimation of the PSF, registration noise due to inaccurate registration and additive Gaussian noise) into consideration. All three types of noise will affect the residual norm of the cost function of each LR frame (channel). The three types of errors can result in different residual noise levels per frame. For example, motion estimation might be more successful for some frames than for others. Furthermore, the system PSF can be different between frames due to time-varying atmospheric turbulence. These situations will lead to different noise levels per LR frame. An iterative process is, thus, proposed with a regularization parameter to control the within-channel balance between received data and prior information, and a channel weight coefficient to control the channel fidelity. The convergence of the proposed algorithm is also fully discussed.

The rest of the paper is organized as follows. In Section II, a regularized cost function for super-resolution (resolution enhancement) is proposed. An iterative algorithm is derived along with the proof of convergence and choice of the regularization parameter and channel weight coefficients. In Section III, experimental results and a comparison of the proposed algorithm with five other methods are presented. Finally, in Section IV, conclusions are drawn and future work is suggested.

II. Regularized Cost Function for Resolution Enhancement

A. Observation Model

The image degradation process is modeled by a linear blur, motion, subsampling by pixel averaging along with additive Gaussian noise. We assume that p LR images, each of size $N_1 \times N_2$, are obtained from the acquisition process. The following observation model is assumed, where all images are ordered lexicographically [11], [13], [24]

$$\mathbf{y} = \mathbf{W}\mathbf{z} + \mathbf{n}. \tag{1}$$

The full set of LR frames is described as $\mathbf{y} = \left[\mathbf{y}_1^T, \mathbf{y}_2^T, \ldots, \mathbf{y}_p^T\right]^T$, where $\mathbf{y}_k$, $k = 1, \ldots p$, are the p LR images. The desired HR image $\mathbf{z}$ is of size $N = l_1 N_1 \times l_2 N_2$, where l_1 and l_2 represent the up-sampling factors in the horizontal and vertical directions, respectively. The term $\mathbf{n}$ represents zero-mean additive Gaussian noise.

In (1), the degradation matrix $\mathbf{W} = [\mathbf{W}_1, \mathbf{W}_2, \ldots, \mathbf{W}_k]^T$ performs the operations of blur, motion and subsampling. Thus, $\mathbf{W}_k$ for frame k can be further written as

$$\mathbf{W}_k = \mathbf{S}\mathbf{B}_k\mathbf{M}_k \tag{2}$$

where $\mathbf{S}$ is the $N_1 N_2 \times N$ subsampling matrix, $\mathbf{B}_k$ is the $N \times N$ blurring matrix, and $\mathbf{M}_k$ is the $N \times N$ motion matrix which consists of 0s and 1s and gives the location of each pixel after motion. In this paper, we assume that no information is lost or added due to motion operation, and matrix $\mathbf{M}_k$ indicates the "new" location of each pixel of frame k on the HR grid after motion operation, with respect to the original HR image. In this case, the elements of the motion matrix are 0s and 1s, with only one 1 in each column and each row. This corresponds to translational motion. We can easily verify that $\mathbf{M}_k$ is a unitary matrix ($\mathbf{M}_k^T\mathbf{M}_k = \mathbf{I}$, where $\mathbf{I}$ is the $N \times N$ identity matrix).

The observation model for each frame can be written as

$$\mathbf{y}_k = \mathbf{W}_k\mathbf{z} + \mathbf{n}_k \tag{3}$$

for $k = 1, \ldots, p$. $\mathbf{n}_k$ represents zero-mean additive noise.

B. Cost Function

A regularized approach using the image prior information of the desired HR image can be used to make the inverse problem well-posed. Considering that each LR image may experience a different degradation process, which implies that different weighting should be given to it in the desired solution, the following channel-weighted cost function is proposed

$$L(\mathbf{z}) = \sum_{k=1}^{p} c_k L_k[\alpha_k(\mathbf{z}), \mathbf{z}] \tag{4}$$

where c_k is the positive weight coefficient for channel k and

$$L_k[\alpha_k(\mathbf{z}), \mathbf{z}] = \|\mathbf{y}_k - \mathbf{W}_k\mathbf{z}\|^2 + \alpha_k(\mathbf{z})\|\mathbf{D}\mathbf{z}\|^2 \tag{5}$$

Authorized licensed use limited to: University of Ioannina. Downloaded on November 19, 2009 at 08:29 from IEEE Xplore. Restrictions apply.

where the operator $\mathbf{D}$ is generally a high-pass filter and is used to penalize discontinuities in the final solution. The regularization parameters $\alpha_k(\mathbf{z})$ control the relative contribution between the error term for the kth channel (residual norm $||\mathbf{y}_k - \mathbf{W}_k\mathbf{z}||^2$) and the smoothness norm $||\mathbf{D}\mathbf{z}||^2$. In this paper, we still use the L_2 norm instead of the L_1 norm that was used in [22], [23].

In this deterministic regularization formulation, the usage of the L_2 norm does not imply that the distribution of noise is exactly of Gaussian type. When the noise power is well bounded in most regions, we believe that the L_2 norm is still a good selection. The justification that the residual noise is approximately Gaussian is provided in the Appendix. In the overall cost function (4), the individual cost functions (5) are weighted by c_k, which denotes the importance and usefulness of the channel information. If the information of each channel is assumed to be equally important, all c_ks can be simply set to be 1. In this special case, the overall cost function (4) will be reduced to that in [25]. However, due to the difference among the channels, the residual norm $||\mathbf{y}_k - \mathbf{W}_k\mathbf{z}||^2$ for each channel k may be different from channel to channel. Thus, the weighted form of the overall cost function applies to more general cases. Here, the residual norm $||\mathbf{y}_k - \mathbf{W}_k\mathbf{z}||^2$ has three possible sources: PSF blur noise, registration noise and additive Gaussian noise, but as we will show later, the channel weights can adaptively balance the contributions from the p channels.

C. Choice of Regularization Parameter

In order for the nonlinear cost function $L(\mathbf{z})$ to have a global minimum, $\alpha_k(\mathbf{z})$ should be chosen in a proper way. Also, compared with the cost function in [25], now each individual channel cost function is weighted by c_k, which corresponds to the reliability of a specific channel. In the following, we expand the choice in [25] to a more general case, where each individual cost function is assigned a weight coefficient c_k. There are many meaningful choices of the regularization parameter. In this paper, the following propositions and properties are adapted from [26].

Proposition 1: Positive weighted summation of convex functional results in a convex function. The convexity of an individual cost function implies (for simplicity, we drop the $\alpha_k(\mathbf{z})$ from the cost function $L_k[\mathbf{z}]$)

$$L_k[\lambda\mathbf{z}_1 + (1-\lambda)\mathbf{z}_2] \geq \lambda L_k[\mathbf{z}_1] + (1-\lambda)L_k[\mathbf{z}_2] \quad (6)$$

for $k = 1, \ldots, p$, $\mathbf{z}_1, \mathbf{z}_2 \in \lfloor Re^{N\times 1}$ and $0 \leq \lambda \leq 1$. This proposition can be proved by multiplying both sides of the above inequality with the positive weight coefficient c_k and summing up. Therefore, if each individual cost function $L_k[\alpha_k(\mathbf{z}), \mathbf{z}]$ in (5) is convex, the cost function in (4) is also convex.

Now, the regularization parameter should be selected in the way such that each individual cost function is convex and the regularization parameter is able to control the balance between the residual norm $||\mathbf{y}_k - \mathbf{W}_k\mathbf{z}||^2$ and the smoothness norm $||\mathbf{D}\mathbf{z}||^2$. Thus, we impose the following desirable properties for $\alpha_k(\mathbf{z})$:

Property 1:

$$\alpha_k(\mathbf{z}) = f(L_k[\alpha_k(\mathbf{z}), \mathbf{z}]) = \gamma_k\{L_k[\alpha_k(\mathbf{z}), \mathbf{z}]\} \quad (7)$$

or, equivalently

$$\alpha_k(\mathbf{z}) = \frac{||\mathbf{y}_k - \mathbf{W}_k\mathbf{z}||^2}{\frac{1}{\gamma_k} - ||\mathbf{D}\mathbf{z}||^2} \quad (8)$$

where $f(\cdot)$ represents a linear monotonically increasing function. The justification behind this choice is based on the set theoretic formulation of the restoration problem [7], [26] and we have also observed that it gives good results. The smaller the smoothness norm $||\mathbf{D}\mathbf{z}||^2$, the more energy is distributed to the low frequency components in the partially reconstructed HR image and a relatively smaller regularization parameter can be used to further recover high frequency components of the HR image, and vice versa. Therefore, $\alpha_k(\mathbf{z})$ should be proportional to both the residual norm $||\mathbf{y}_k - \mathbf{W}_k\mathbf{z}||^2$ and smoothness norm $||\mathbf{D}\mathbf{z}||^2$. Also, for a linear $f(\cdot)$, the minimizer $\hat{\mathbf{z}}$, which satisfies $\bigtriangledown_{\mathbf{z}} L(\hat{\mathbf{z}}) = 0$, also satisfies $\bigtriangledown_{\mathbf{z}} \sum_{k=1}^{p} c_k\alpha_k(\hat{\mathbf{z}}) = 0$

$$\begin{aligned} 0 &= \frac{df}{dL} \cdot \bigtriangledown_{\mathbf{z}} L(\hat{\mathbf{z}}) \\ &= \left[\frac{df(L)}{d\mathbf{z}}\right]_{\mathbf{z}=\hat{\mathbf{z}}} \\ &= \bigtriangledown_{\mathbf{z}} f\left\{\sum_{k=1}^{p} c_k L_k[\alpha_k(\hat{\mathbf{z}}), \hat{\mathbf{z}}]\right\} \\ &= \bigtriangledown_{\mathbf{z}} \sum_{k=1}^{p} c_k f\{L_k[\alpha_k(\hat{\mathbf{z}}), \hat{\mathbf{z}}]\} \\ &= \bigtriangledown_{\mathbf{z}} \sum_{k=1}^{p} c_k\alpha_k(\hat{\mathbf{z}}). \end{aligned} \quad (9)$$

Property 2: The $\alpha_k(\mathbf{z})$ should be chosen to make $L_k[\alpha_k(\mathbf{z}), \mathbf{z}]$ convex. The sufficient condition for this is [7]

$$\frac{\partial f(L_k)}{\partial L_k} \leq \frac{1}{||\mathbf{D}\mathbf{z}||^2}. \quad (10)$$

From Proposition 1, $L(\mathbf{z})$ is also convex and the local minimizer will also become the global minimizer. Also from (7) and (10), the condition for convexity can be derived as $(1/\gamma_k) > ||\mathbf{D}\mathbf{z}||^2$, which ensures a positive $\alpha_k(\mathbf{z})$ in (8).

With the given properties, the gradient of the cost function $L(\mathbf{z})$ is

$$\begin{aligned} \bigtriangledown_{\mathbf{z}} L(\mathbf{z}) &= 2\sum_{k=1}^{p} c_k \left\{\left[\mathbf{W}_k^T\mathbf{W}_k + \alpha_k(\mathbf{z})\mathbf{D}^T\mathbf{D}\right]\mathbf{z} \right. \\ &\qquad \left. -\mathbf{W}_k^T\mathbf{y_k} + ||\mathbf{D}\mathbf{z}||^2 \bigtriangledown_{\mathbf{z}} \alpha_k(\mathbf{z})\right\} \\ &= 2\sum_{k=1}^{p} c_k \left\{\left[\mathbf{W}_k^T\mathbf{W}_k + \alpha_k(\mathbf{z})\mathbf{D}^T\mathbf{D}\right]\mathbf{z} - \mathbf{W}_k^T\mathbf{y_k}\right\} \\ &\quad + 2||\mathbf{D}\mathbf{z}||^2 \sum_{k=1}^{p} c_k \bigtriangledown_{\mathbf{z}} \alpha_k(\mathbf{z}). \end{aligned} \quad (11)$$

At the global minimum, the gradient is equal to the zero vector. According to (9), the last term of (11) becomes zero at the minimizer. The HR image is the solution of

$$\sum_{k=1}^{p} c_k \left[\mathbf{W}_k^T\mathbf{W}_k + \alpha_k(\mathbf{z})\mathbf{D}^T\mathbf{D}\right]\mathbf{z} = \sum_{k=1}^{p} c_k \left[\mathbf{W}_k^T\mathbf{y_k}\right] \quad (12)$$

Authorized licensed use limited to: University of Ioannina. Downloaded on November 19, 2009 at 08:29 from IEEE Xplore. Restrictions apply.

and can be solved using iterative method

$$\hat{\mathbf{z}}_{n+1} = \hat{\mathbf{z}}_n - \epsilon \sum_{k=1}^{p} c_k \left\{ \left[\mathbf{W}_k^T \mathbf{W}_k + \alpha_k(\mathbf{z}) \mathbf{D}^T \mathbf{D} \right] \hat{\mathbf{z}}_n - \mathbf{W}_k^T \mathbf{y_k} \right\}. \quad (13)$$

The sufficient condition for the convergence of the above iteration is given by the following proposition [25].

Proposition 2: Consider the equation

$$G(\mathbf{z})\mathbf{z} = \mathbf{b} \quad (14)$$

where $G(\mathbf{z})$ is a matrix, $G(\mathbf{z}) = c_1 G_1(\mathbf{z}) + c_2 G_2(\mathbf{z}) + \cdots + c_p G_p(\mathbf{z})$, $\mathbf{b} = c_1\mathbf{b}_1 + c_2\mathbf{b}_2 + \cdots + c_p\mathbf{b}_p$, $c_1, c_2, \ldots, c_p$ are positive coefficients and each $c_k G_k(\mathbf{z})$ is a positive definite matrix. The sufficient condition for the convergence of iteration

$$\hat{\mathbf{z}}_{n+1} = \hat{\mathbf{z}}_n - \epsilon[G(\hat{\mathbf{z}}_n)\hat{\mathbf{z}}_n - \mathbf{b}] \quad (15)$$

is

$$\epsilon \cdot \phi_{\max}[J_{c_k G_k(\mathbf{z})\mathbf{z}}] < \frac{2}{p} \quad (16)$$

where $J_{c_k G_k(\mathbf{z})\mathbf{z}}$ is the Jacobian matrix of vector $c_k G_k(\mathbf{z})\mathbf{z}$ and $\phi_{\max}(\cdot)$ is the maximum singular value of a matrix. Equivalently, because of the positivity of c_k along with the assumption that c_k is not a function of $\mathbf{z}$, the above inequality can be rewritten as

$$\epsilon \cdot \phi_{\max}[J_{G_k(\mathbf{z})\mathbf{z}}] < \frac{2}{p}. \quad (17)$$

For subsampling by pixel averaging in (2), we can easily verify that $\mathbf{S}\mathbf{S}^T = (1/(l_1 l_2))\mathbf{I}$, where $\mathbf{I}$ is the $N_1 N_2 \times N_1 N_2$ identity matrix. Therefore, $\phi_{\max}[\mathbf{S}^T\mathbf{S}] = \phi_{\max}[\mathbf{S}\mathbf{S}^T] = (1/(l_1 l_2))$; also, from the earlier discussion, we know $\mathbf{M}$ is a unitary matrix. Therefore, $\mathbf{M}_k^T\mathbf{M}_k = \mathbf{I}$. Further, the impulse response coefficients of the PSF are assumed to be normalized to add to 1; thus, $\phi\left(\mathbf{B}_k^T\mathbf{B}_k\right) = 1$ [13]. By applying Proposition 2 and (2) to (13) and using the property of singular value of a matrix, we have

$$\begin{aligned}
&\phi_{\max}\left[\mathbf{W}_k^T\mathbf{W}_k + \alpha_k(\mathbf{z})\mathbf{D}^T\mathbf{D}\right] \\
&\quad \le \phi_{\max}\left[\mathbf{W}_k^T\mathbf{W}_k\right] + \alpha_k(\mathbf{z})\phi_{\max}[\mathbf{D}^T\mathbf{D}] \\
&\quad = \phi_{\max}\left[\mathbf{B}_k^T\mathbf{M}_k^T\mathbf{S}^T\mathbf{S}\mathbf{M}_k\mathbf{B}_k\right] + \alpha_k(\mathbf{z})\phi_{\max}[\mathbf{D}^T\mathbf{D}] \\
&\quad \le \phi_{\max}\left[\mathbf{B}_k^T\right]\phi_{\max}\left[\mathbf{M}_k^T\right]\phi_{\max}[\mathbf{S}^T]\phi_{\max} \\
&\qquad \times [\mathbf{S}]\phi_{\max}[\mathbf{M}_k]\phi_{\max}[\mathbf{B}_k] \\
&\qquad + \alpha_k(\mathbf{z})\phi_{\max}\left[\mathbf{D}^T\mathbf{D}\right] \\
&\quad = \phi_{\max}[\mathbf{B}_k^T\mathbf{B}_k]\phi_{\max}\left[\mathbf{M}_k^T\mathbf{M}_k\right]\phi_{\max}[\mathbf{S}^T\mathbf{S}] \\
&\qquad + \alpha_k(\mathbf{z})\phi_{\max}[\mathbf{D}^T\mathbf{D}] \\
&\quad = \frac{1}{(l_1 l_2)} + \alpha_k(\mathbf{z})\phi_{\max}[\mathbf{D}^T\mathbf{D}] \\
&\quad < \frac{2}{\epsilon p}.
\end{aligned} \quad (18)$$

Therefore

$$\alpha_k(\mathbf{z}) < \frac{2 - \epsilon p \frac{1}{(l_1 l_2)}}{\epsilon p \phi_{\max}[\mathbf{D}^T\mathbf{D}]}. \quad (19)$$

From (8) and (19), we have

$$\frac{1}{\gamma_k} < \frac{\epsilon p \phi_{\max}[\mathbf{D}^T\mathbf{D}]}{2 - \epsilon p (l_1 l_2)} ||\mathbf{y}_k - \mathbf{W}_k\mathbf{z}||^2 + ||\mathbf{D}\mathbf{z}||^2. \quad (20)$$

If we can select the step size ϵ as

$$\epsilon = \frac{2}{p}\left(\frac{l_1 l_2}{(l_1 l_2)\phi_{\max}[\mathbf{D}^T\mathbf{D}] + 1}\right) \quad (21)$$

inequality (20) will become

$$\frac{1}{\gamma_k} < ||\mathbf{y}_k - \mathbf{W}_k\mathbf{z}||^2 + ||\mathbf{D}\mathbf{z}||^2. \quad (22)$$

An upper bound of $(1/\gamma_k)$ is $(1 + l_1 l_2)||\mathbf{y}_k||^2$, since $||\mathbf{y}_k - \mathbf{W}_k\mathbf{z}||^2 < ||\mathbf{y}_k||^2$ (each LR image is assumed to have more energy than the residual noise), and $||\mathbf{D}\mathbf{z}||^2 < ||\mathbf{z}||^2 \approx l_1 l_2 ||\mathbf{y}_k||^2$. Considering piece-wise smoothness of $\mathbf{z}$, usually $||\mathbf{D}\mathbf{z}||^2 < (||\mathbf{z}||^2/l_1 l_2) \approx ||\mathbf{y}_k||^2$ is satisfied for not too large upsampling ratio l_1, l_2. Therefore, we use $(1/\gamma_k) = 2||\mathbf{y}_k||^2$ in this paper and [13], which is shown to be a good choice in the experimental results.

D. Adaptive Update of Channel Weights

The channel weight c_k is the indicator of the reliability of each channel. Channels with larger residual noise should be given relatively smaller weight.

There are three sources for the residual noise: 1) Type I: PSF blur noise due to nonperfect estimation of the PSF; 2) Type II: registration noise, due to the nonperfect estimation of the registration parameters; 3) Type III: AWGN. All three types of noise contribute to the residual norm $||\mathbf{y}_k - \mathbf{W}_k\mathbf{z}||^2$, the first term in the cost function for each channel. We assume that this residual norm depends on the registration and PSF estimation errors as well as the additive noise and is not directly related to the HR image $\mathbf{z}$. In most previous work, only Type III noise is taken into account, and assumed to be independent and identically distributed (i.i.d). In this case, all the channels are given equal weight $c_k = 1$. In our recent work [24], Type III noise with different noise levels for each channel is taken into consideration. In [19], Type II noise is also modeled as Gaussian-type noise and an adaptive regularization algorithm is proposed.

Based on the the justification provided in the Appendix, the residual noise is assumed to be approximately Gaussian. If the noise variance for channel k is σ_k^2 and the residual norm of channel k is bounded by $\sigma_k^2 N_1 N_2$, we propose that the channel weight c_k should satisfy the following properties: (a) the c_k should be inversely proportional to the residual norm $||\mathbf{y}_k - \mathbf{W}_k\mathbf{z}||^2$; (b) $\sum_{k=1}^{p} c_k = p$. This constraint avoids the trivial solution (all zeros) for c_k. The simplest linear solution for criteria (a) and (b) is

$$c_k = \frac{R_{\text{ave}}}{||\mathbf{y}_k - \mathbf{W}_k\mathbf{z}||^2} \quad (23)$$

where R_{ave} is the average residual norm defined as

$$R_{\text{ave}} = \frac{p}{\sum_{k=1}^{p} \frac{1}{||\mathbf{y}_k - \mathbf{W}_k\mathbf{z}||^2}}. \quad (24)$$

Authorized licensed use limited to: University of Ioannina. Downloaded on November 19, 2009 at 08:29 from IEEE Xplore. Restrictions apply.

We can see that c_k is actually an inversely factored estimator of the "Gaussian" bound σ_k^2. Note that more complex solutions for c_k can be obtained using nonlinear functions, such as logarithmic function. Compared with the methods of Lee and Kang, the major difference is that in out method, the smoothness norm $||\mathbf{Dz}||^2$ is bounded. The proper bound $(1/\gamma_k)$ not only prevents the possibility of exponential increase of the regularization functional in this ill-posed problem, but also adaptively enhances the imagery detail. When the smoothness norm $||\mathbf{Dz}||^2$ is smaller, which means that the HR image consists of more low-frequency components, a relatively small α_k is provided to let enough high-frequency components appear in the reconstructed HR image. This is why our method will give better result than those of Lee and Kang in general.

We also notice that the convergence of Lee–Kang's method is not mathematically verified and some choices of the regularization functional of the regularization parameters will exponential increase during the reconstruction and not converge. In our method, the convergence is always guaranteed and the relationship between c_k and α_k is more clear. Also, our method is already in multichannel form and can be computed in parallel.

c_k depends on the residual norm, which is assumed to be a function of the three types of noise and has little dependence on the particular $\mathbf{z}$. Thus, c_k is assumed to be a constant. Therefore, the derivations regarding convergence in the previous section still hold. Now, the weight coefficients in (8) work as the cross-channel fidelity, while the regularization parameter in (23) acts as the within-channel balance between data and prior model for each channel.

Compared to the choice of regularization parameters in paper [19], our method explicitly separates the within-channel balance and cross-channel balance. The regularization is imposed on each channel instead of on the overall weighted-channel residual norm. Our method is able to find the unreliable channels and gives them less fidelity more quickly because linear solution implemented. By imposing property (b), $\sum_{k=1}^{p} c_k = p$, the proposed method also avoids the problem of exponential increase of the regularization parameters for some functionals.

III. Experimental Results

A number of experiments were conducted, some of which are presented here. To test the performance of our algorithms, we used the 256×256 "Cameraman" and "Lena" test images for the synthetic test. Four frames were generated with down-sampling ratio $l_1 = l_2 = 2$. Four cases, Cases 1–4, as listed in Table I, were tested. In these four tests, the PSF was a Gaussian blur with support size 15×15 and STD $\sigma = 1.7$ for the no blur-noise cases (the PSF was assumed to have been perfectly estimated). For blur-noise cases, the PSF estimation was biased and determined to be Gaussian with a STD $\sigma = 1.4$. The registration parameters for the four frames were global translations $[0,0]$, $[0,1]$, $[1,0]$, $[1,1]$ in the HR grid, respectively, for the no registration-noise cases. For registration-noise cases, the second frame's motion vector was biased by one pixel to $[0,2]$. i.i.d. AWGN noise with same variance σ_η^2 was added to each frame, which corresponds to a signal-to-noise ratio (SNR) of 30–40 dB, the same level as the AWGN noise of the real data.

TABLE I
Four Cases of Synthetic Test

	Additive noise	Blur noise	Registration noise
Case 1	Y	N	N
Case 2	Y	N	Y
Case 3	Y	Y	N
Case 4	Y	Y	Y

$\mathbf{D}$ was a high-pass filter formed by the two-dimensional Laplacian kernel defined as

$$d_{i,j} = \begin{cases} 1, & \text{for } i = j \\ -\frac{1}{4}, & \text{for } i,j : z_j \text{ is a cardinal neighbor of } z_i. \end{cases} \quad (25)$$

To compare, we test the four cases in Table I and list the results from the proposed algorithm along with five other algorithms, that is, bilinear Interpolation, algorithm of Hardie [11] with the best visual reconstruction (the regularization parameter was obtained via trial and error), algorithm (I) of Lee–Kang [19], algorithm (II) of Lee–Kang [19], and, simultaneous method without weighted channels [13]. Since the algorithms of Lee–Kang do not consider inaccurate PSF estimate, results for these algorithms are only presented for Cases 1 and 2.

Each algorithm was carried out until convergence was reached when $((\|\hat{\mathbf{z}}^{n+1} - \hat{\mathbf{z}}^n\|)/(\|\hat{\mathbf{z}}^n\|)) < 10^{-6}$. The peak signal to noise ratio (PSNR) values of the reconstructed images for "Cameraman" and "Lena" using the six methods are shown in Tables II and III, respectively. The reconstructed HR images of for "Cameraman" and "Lena" using the six methods in Case 2 are shown in Figs. 1–6 and Figs. 7–12, respectively.

From Tables II and III, it can be seen that the "nonchannel-weighted simultaneous method" provides a better or close reconstruction compared to the algorithm of Hardie in Case 1, as has been shown in [13]. For Cases 2, 3, and 4, when there exist inaccurate estimates of PSF blur and/or registration, Hardie's method with a good regularization parameter may perform better than "nonchannel-weighted simultaneous method," but when adaptive channel weighting is utilized in the proposed method, it provides the best PSNR values among the algorithms.

Also, when the adaptive channel weighting is utilized, the proposed method performs better than both algorithms of Lee–Kang, in the sense of the average enhanced PSNR values for Cases 1 and 2 by 0.475 and 0.310 dB for the "Cameraman" and 0.690 and 0.535 dB for the "Lena," respectively. From these results, we can see that our algorithm is applicable to different cases of noise and generates good reconstruction results.

Furthermore, we can see that for the "Cameraman," the proposed algorithm has an average PSNR improvement of 0.340 dB compared to the simultaneous method without weighted channels for the two registration-noise cases (Cases 2 and 4), and 0.235-dB PSNR improvement for the two blur-noise

Authorized licensed use limited to: University of Ioannina. Downloaded on November 19, 2009 at 08:29 from IEEE Xplore. Restrictions apply.

Fig. 1. Bilinear interpolation of the first LR Cameraman image in Case 2.

Fig. 2. Reconstructed HR Cameraman image using Hardie's algorithm in Case 2.

Fig. 3. Reconstructed HR Cameraman image using Lee–Kang's algorithm (I) in Case 2.

cases (Cases 3 and 4). These improvements for "Lena" are 0.525 and 0.345 dB, respectively. This indicates that Type II noise has a more serious effect during the process of HR reconstruction than Type I noise, which shows the need for accurate registration, which is more important than the perfect estimation of the PSF of the optical lens.

Fig. 4. Reconstructed HR Cameraman image using Lee–Kang's algorithm (II) in Case 2.

Fig. 5. Reconstructed HR Cameraman image using the simultaneous method without weighted channels in Case 2.

Fig. 6. Reconstructed HR Cameraman image using the proposed method in Case 2.

It is also easy to see that when only AWGN noise exists (Case 1), the reconstruction result from the proposed algorithm is equivalent to that in [24].

Next, we used real data of two video sequences provided to us by the Naval Research Laboratory, Washington, DC, to test

Authorized licensed use limited to: University of Ioannina. Downloaded on November 19, 2009 at 08:29 from IEEE Xplore. Restrictions apply.

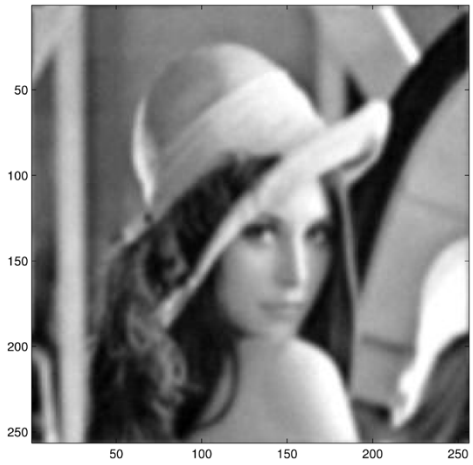

Fig. 7. Bilinear interpolation of the first LR Lena image in Case 2.

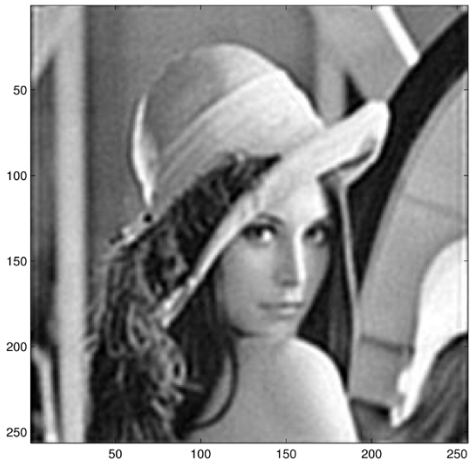

Fig. 8. Reconstructed HR Lena image using Hardie's algorithm in Case 2.

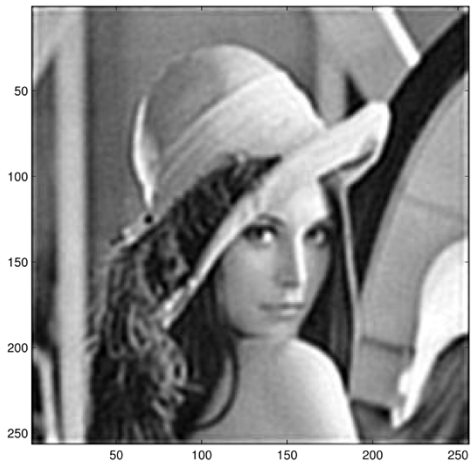

Fig. 9. Reconstructed HR Lena image using Lee–Kang's algorithm (I) in Case 2.

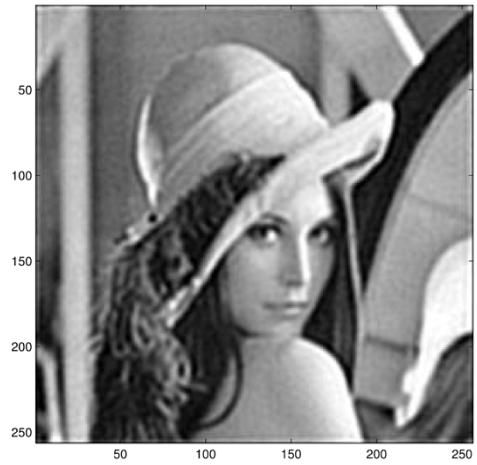

Fig. 10. Reconstructed HR Lena image using Lee–Kang's algorithm (II) in Case 2.

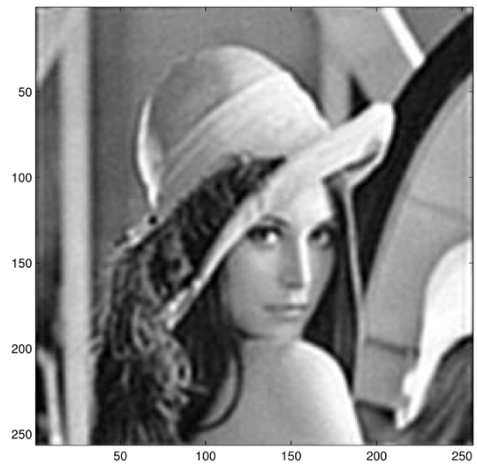

Fig. 11. Reconstructed HR Lena image using simultaneous method without weighted channels in Case 2.

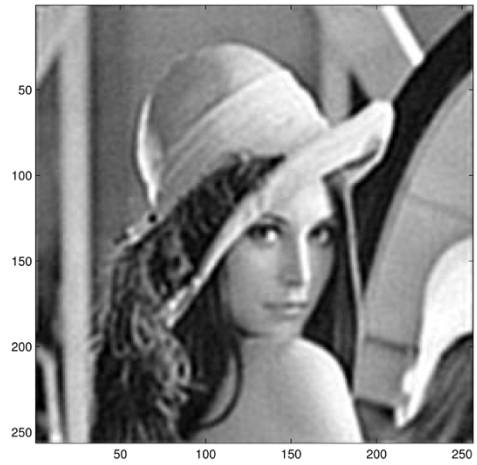

Fig. 12. Reconstructed HR Lena image using the proposed method in Case 2.

the proposed algorithm. The first sequence is infrared and consists of 20 frames of the LR "truck" image with size 128×128 pixels. The second sequence consists of 16 frames of the LR "chart" image with size 64×64 pixels. The up-sampling ratio is $l_1 = l_2 = 4$. We assumed a Gaussian PSF for the lens and estimated its STD at 1.7 using trial and error. Bilinear interpolation of the first frame was chosen as the first estimate of HR image $\mathbf{z}$. Registration parameters were predetermined for each 16×16 macro block on the HR grid using the optical flow

Authorized licensed use limited to: University of Ioannina. Downloaded on November 19, 2009 at 08:29 from IEEE Xplore. Restrictions apply.

TABLE II
RESULTS OF "CAMERAMAN" USING THE SIX METHODS

PSNR (dB)	Bilinear	Algorithm of Hardie	Algorithm (I) of Lee-Kang	Algorithm (II) of Lee-Kang	Simultaneous Method without weighted channels	Proposed Method
Case 1	22.51	24.90	24.54	24.60	24.92	24.92
Case 2	22.51	24.64	24.32	24.59	24.59	24.89
Case 3	22.51	24.75	-	-	24.68	24.77
Case 4	22.52	24.38	-	-	24.36	24.74

TABLE III
RESULTS OF "LENA" USING THE SIX METHODS

PSNR (dB)	Bilinear	Algorithm of Hardie	Algorithm (I) of Lee-Kang	Algorithm (II) of Lee-Kang	Simultaneous Method without weighted channels	Proposed Method
Case 1	24.97	27.81	27.29	27.28	27.83	27.83
Case 2	24.96	27.37	26.95	27.27	27.30	27.79
Case 3	24.96	27.47	-	-	27.36	27.59
Case 4	24.96	26.97	-	-	26.98	27.54

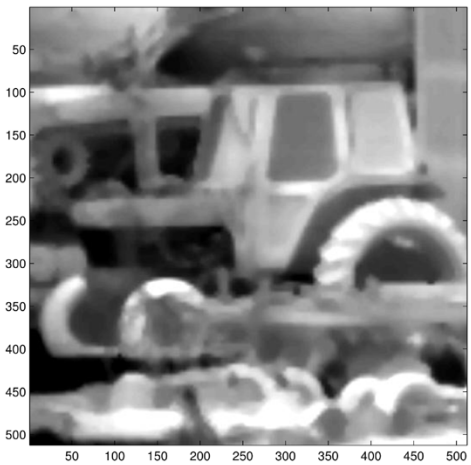

Fig. 13. Bilinear interpolation of the first frame of truck sequence.

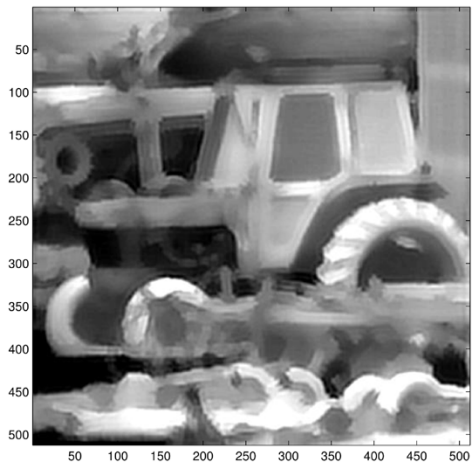

Fig. 14. Reconstructed HR truck image using simultaneous method without weighted channels.

method [16]. We assumed that convergence was reached when $((((\|\hat{\mathbf{z}}^{n+1} - \hat{\mathbf{z}}^{n}\|)/(\|\hat{\mathbf{z}}^{n}\|))) < 10^{-6}$.

The reconstructions using the six methods for "truck" sequence are shown in Fig. 13–18, respectively. The proposed method provides the sharpest reconstruction among the algorithms.

The reconstructions using the six methods for "chart" sequence are shown in Figs. 19–24, respectively. The bars in the reconstruction using the proposed method are sharper and easily decided to be horizontal or vertical.

We also test the a underdetermined system using "chart" with ten frames. The reconstruction using the proposed method is shown in Fig. 25. The availability of fewer frames blurs the detailed information of some smaller bars, but the overall quality of the reconstruction is still good, with most bars easily decided horizontal or vertical.

In all the experimental tests, the computational cost of our method is lower than that of Hardie and Lee–Kang methods, because a fixed step size is used in the proposed method instead of updating the step size in their methods. The computational cost of the proposed method is higher than that of "non-channel-weighted simultaneous method" because of channel weighting, but this increase is reasonable considering the much better PSNR values provided by the proposed method, for cases with inaccurate estimates. Compared to the "non-channel-weighted simultaneous method" in our experiments, the methods of Hardie, Lee–Kang algorithm (I), Lee–Kang algorithm (II), and the proposed method are 2.21, 2.19, 2.23, and 1.52 times slower, respectively. Besides the computational issue, the proposed method also provides the highest PSNR values for synthetic images, as well as the best visual quality for real data among the tested algorithms.

Authorized licensed use limited to: University of Ioannina. Downloaded on November 19, 2009 at 08:29 from IEEE Xplore. Restrictions apply.

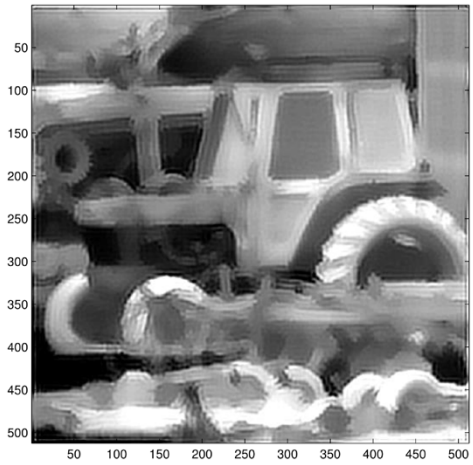

Fig. 15. Reconstructed HR truck image using Hardie's method.

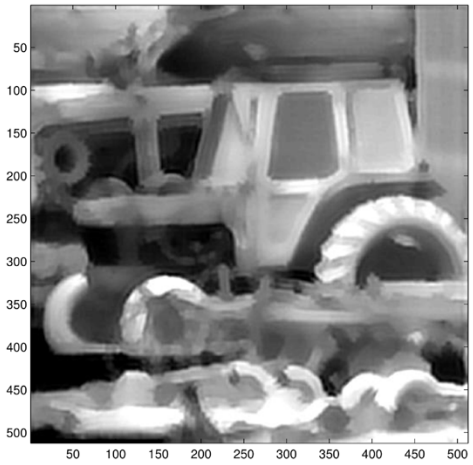

Fig. 16. Reconstructed HR truck image using Lee–Kang's algorithm (I).

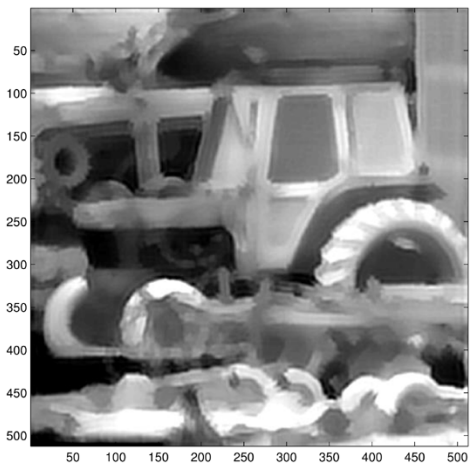

Fig. 17. Reconstructed HR truck image using Lee–Kang's algorithm (II).

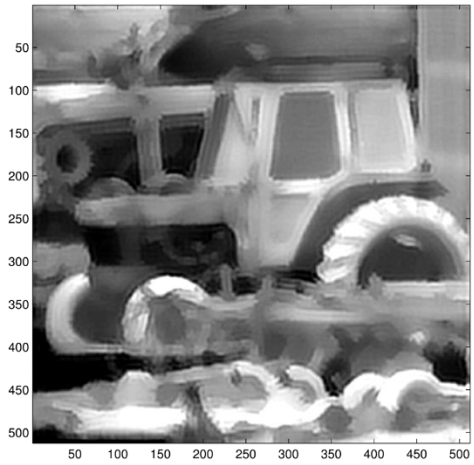

Fig. 18. Reconstructed HR truck image using the proposed method.

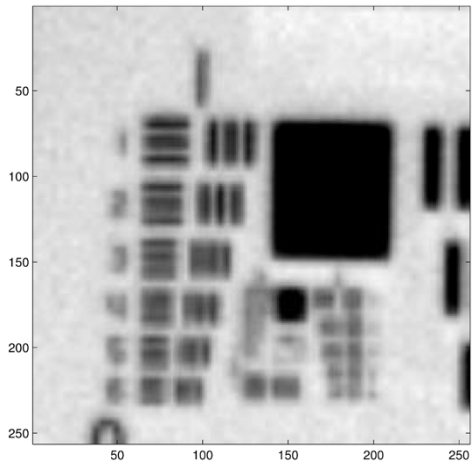

Fig. 19. Bilinear interpolation of the first frame of chart sequence.

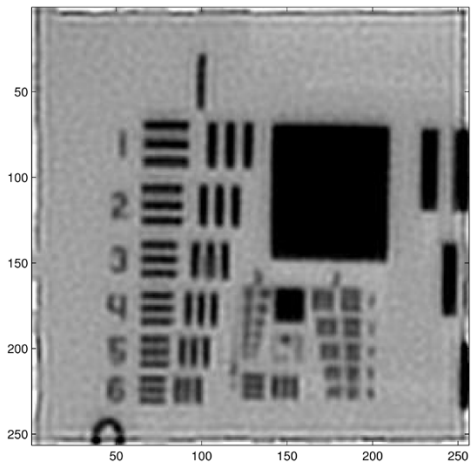

Fig. 20. Reconstructed HR chart image using simultaneous method without weighted channels.

IV. Conclusion

In this paper, we proposed a technique for image super-resolution (resolution enhancement) with adaptively weighted LR frames (channels) and simultaneous estimation of the regularization parameter. The weight coefficients work as the cross-channel fidelity to each LR image, while the regularization parameter acts as the within-channel balance between data and prior model. The convergence property of the proposed algorithm is analyzed in detail. More importantly, experimental results show the validity of our algorithm in cases with inaccurate subpixel registration along with inaccurate estimate of the PSF of the optical system. Also, from results of different noise cases, we conclude that the registration noise (Type II) impairs

Authorized licensed use limited to: University of Ioannina. Downloaded on November 19, 2009 at 08:29 from IEEE Xplore. Restrictions apply.

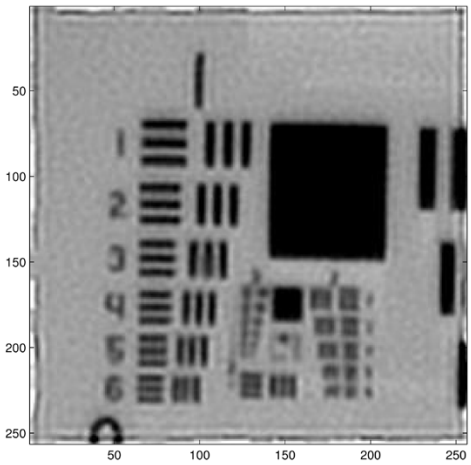

Fig. 21. Reconstructed HR chart image using Hardie's method.

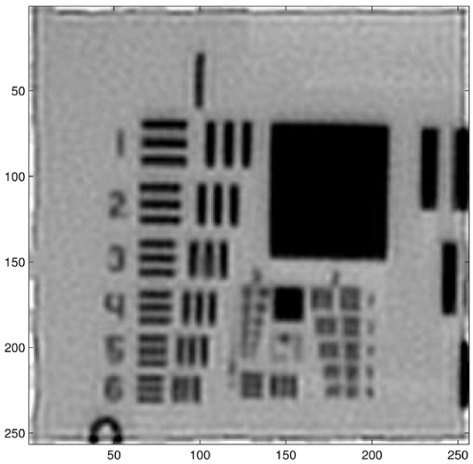

Fig. 22. Reconstructed HR chart image using Lee–Kang's algorithm (I).

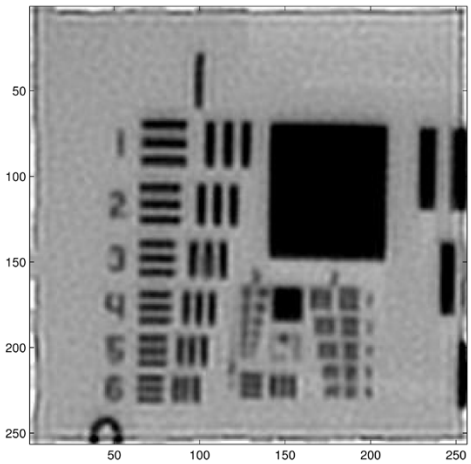

Fig. 23. Reconstructed HR chart image using Lee–Kang's algorithm (II).

the reconstruction quality more compared to the PSF blur noise (Type I).

APPENDIX

In this appendix, we will justify the assumption that the residual noise is approximately Gaussian considering different

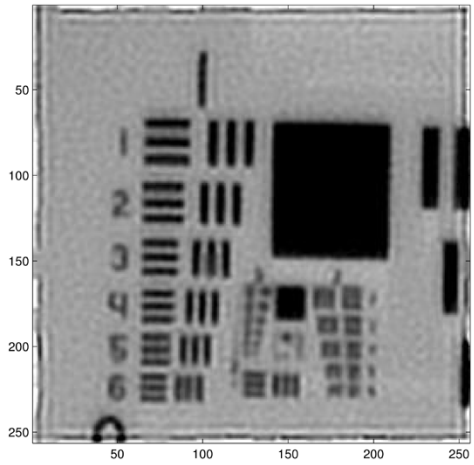

Fig. 24. Reconstructed HR chart image using the proposed method.

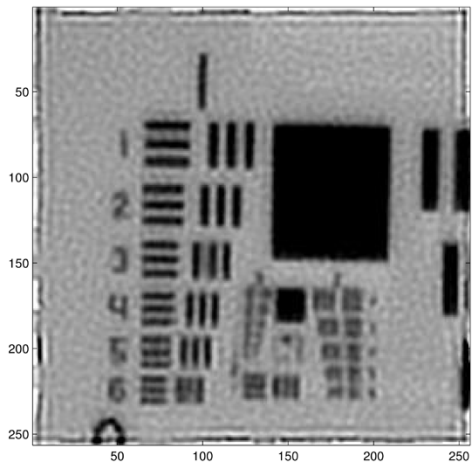

Fig. 25. Reconstructed HR chart image using the proposed method in a underdetermined case.

combinations of the three types of noise. First, let us analyze the distribution of the overall noise to see if it is Gaussian or not. We adapt the GLRT test from [22] to test the residual noise to be nearly Gaussian or Laplacian distributed. When the GLRT score of a random variable, which was simplified to be $(\hat{\sigma}_L/\hat{\sigma}_G)$ in [22], is greater than $(\pi/2e)^{1/2}$, or approximately 0.7602, the random variable is believed to be Gaussian type. Here, $\hat{\sigma}_L$ and $\hat{\sigma}_G$ stand for the ML estimates of the variance when the random variable assumed to be Laplacian distributed or Gaussian distributed, respectively.

In the four synthetic tests listed in Table I, the GLRT scores for "Cameraman" and "Lena" images are as listed in Table IV. In cases 1 and 3, the GLRT scores are higher than 0.7602; thus, the residual noise is more Gaussian than Laplacian. In cases 2 and 4, the GLRT scores are lower than 0.7602; thus, the residual noise is more Laplacian than Gaussian, but we also notice these scores are still close to 0.7602, the threshold GLRT test. Also, we notice that if we just remove a very small percentage of pixels (less than 7%) from the residual image, which have relatively larger absolute value, the GLRT score for the remaining pixels can reach the threshold 0.7602. We call the region of the remaining pixels as "Gaussian" region. It is not surprising to see that the pixels inside of the "Gaussian" region are in the smooth part

Authorized licensed use limited to: University of Ioannina. Downloaded on November 19, 2009 at 08:29 from IEEE Xplore. Restrictions apply.

TABLE IV
TEST OF THE RESIDUAL NOISE OF SYNTHETIC IMAGES

Cameraman	GLRT	Pixel ratio inside of Gaussian region	Gaussian variance	Lena	GLRT	Pixel ratio inside of Gaussian region	Gaussian variance
Case 1	0.7994	100%	17.2270	Case 1	0.7949	100%	22.2016
Case 2	0.5759	94.47%	30.1303	Case 2	0.6540	98.83%	58.8494
Case 3	0.7908	100%	22.9528	Case 3	0.7960	100%	25.6969
Case 4	0.5727	93.91%	31.0734	Case 4	0.6533	97.91%	60.4787

of the HR image, and the the pixels outside of the "Gaussian" region are mainly around the edges of the HR image, which correspond to the high-frequency components. Therefore, in these cases, the residual noise in the smooth region is still approximately Gaussian. The STDs of the "Gaussian" region are also listed in Table IV.

Comparing Case 2 to 1 (or Case 4 to 3), we can see even in the "Gaussian" region only, the noise level is clearly increased (more than 1.5 times) due to the inaccurate estimates. If we consider the "non-Gaussian" edges, the increase of noise level will be even higher. This implies that channel weighting is necessary when there exist different combinations of Type I and Type II noise in the residual norm.

The above findings can be also interpreted from the prior model of the HR image, which is usually taken to be a GMRF. In this prior model, the image consists of piecewise smooth regions, segmented by the edges of objects inside the image. The noise due to inaccurate PSF estimate and/or registration parameter will be equivalent to a high-pass filtering. The larger absolute values of this residual noise happen around the edges of the HR image. The residual noise in the smooth region is still approximately Gaussian type.

REFERENCES

[1] R. Tsai and T. Huang, "Multiframe image restoration and registration," *Adv. Comput. Vis. Image Process.*, vol. 1, pp. 317–339, 1984.

[2] A. M. Tekalp, M. K. Ozkan, and M. I. Sezan, "High-resolution image reconstruction from lower-resolution image sequences and space-varying image restoration," in *Proc. Int. Conf. Acoustics, Speech, Signal Processing*, vol. 3, Mar. 1992, pp. 169–172.

[3] S. P. Kim, N. K. Bose, and H. M. Valenzuela, "Recursive reconstruction of high resolution image from noisy undersampled multiframes," *IEEE Trans. Acoust., Speech, Signal Process.*, vol. 38, no. 6, pp. 1013–1027, Jun. 1990.

[4] H. Stark and P. Oskoui, "High-resolution image recovery from image-plane arrays, using convex projections," *J. Opt. Soc. Amer. A*, vol. 6, pp. 1715–1726, Nov. 1989.

[5] A. J. Patti, M. I. Sezan, and A. M. Tekalp, "Super-resolution video reconstruction with arbitrary sampling lattices and nonzero apperature time," *IEEE Trans. Image Process.*, vol. 6, no. 8, pp. 1064–1076, Aug. 1997.

[6] P. E. Erem, M. I. Sezan, and A. M. Tekalp, "Robust, object-based high-resolution image reconstruction from low-resolution video," *IEEE Trans. Image Process.*, vol. 6, no. 10, pp. 1446–1451, Oct. 1997.

[7] B. C. Tom and A. K. Katsaggelos, "Reconstruction of a high-resolution image from multiple degraded mis-registered low-resolution images," in *Proc. Conf. Visual Communications and Image Processing*, vol. 2308, Sep. 1994, pp. 971–981.

[8] R. R. Schultz and R. L. Stevenson, "A bayesian approach to image expansion for improved definition," *IEEE Trans. Image Process.*, vol. 3, no. 5, pp. 233–242, May 1994.

[9] ——, "Extraction of high-resolution frames from video sequences," *IEEE Trans. Image Process.*, vol. 5, no. 6, pp. 996–1011, Jun. 1996.

[10] ——, "Improved definition video frame enhancement," in *Proc. IEEE Int. Conf. Acoustics, Speech, Signal Processing*, vol. 4, May 1995, pp. 2169–2171.

[11] R. C. Hardie, K. J. Barnard, and E. E. Armstrong, "Joint MAP registration and high-resolution image estimation using a sequence of undersampled images," *IEEE Trans. Image Process.*, vol. 6, no. 12, pp. 1621–1633, Dec. 1997.

[12] L. P. Kondi, D. Scribner, and J. Schuler, "A comparison of digital image resolution enhancement techniques," in *Proc. SPIE AeroSense Conf.*, vol. 4719, Apr. 2002, pp. 220–229.

[13] H. He and L. P. Kondi, "Resolution enhancement of video sequences with simultaneous estimation of the regularization parameter," *J. Electron. Imag.*, vol. 13, pp. 586–596, Jul. 2004.

[14] ——, "Resolution enhancement of video sequences with simultaneous estimation of the regularization parameter," *Proc. SPIE Electron. Imag.*, vol. 5022, pp. 1123–1133, Jan. 2003.

[15] ——, "MAP based resolution enhancement of video sequences using a Huber–Markov random field image prior model," in *IEEE Int. Conf. Image Processing*, vol. 2, 2003, pp. 933–936.

[16] A. M. Tekalp, *Digital Video Processing*. Englewood Cliffs, NJ: Prentice-Hall, 1995.

[17] N. P. Galatsanos and A. K. Katsaggelos, "Methods for choosing the regularization parameter and estimating the noise variance in image restoration and their relation," *IEEE Trans. Image Process.*, vol. 1, no. 1, pp. 322–336, Jul. 1992.

[18] P. C. Hansen, "Rank-deficient and discrete ill-posed problems," *SIAM*, 1997.

[19] E. S. Lee and M. G. Kang, "Regularized adaptive high-resolution image reconstruction considering inaccurate subpixel registration," *IEEE Trans. Image Process.*, vol. 12, no. 7, pp. 826–837, Jul. 2003.

[20] N. P. Galatsanos, V. Z. Mesarovic, R. Molina, and A. K. Katsaggelos, "Hierarchical bayesian image restoration from partially known blurs," *IEEE Trans. Image Process.*, vol. 9, no. 10, pp. 1784–1797, Oct. 2000.

[21] A. Zomet, A. Rav-Acha, and S. Peleg, "Robust super-resolution," in *Proc. Int. Conf. Computer Vision and Patern Recognition*, vol. 1, Dec. 2001, pp. 645–650.

[22] S. Farsiu, D. Robinson, M. Elad, and P. Milanfar, "Robust shift and add approach to super-resolution," in *Proc. SPIE Conf. Applications Digital Signal Image Processing*, vol. 5203, Aug. 2003, pp. 121–130.

[23] ——, "Fast and robust multi-frame super-resolution," *IEEE Trans. Image Process.*, vol. 13, no. 10, pp. 1327–1344, Oct. 2004.

[24] H. He and L. P. Kondi, "Resolution enhancement of video sequences with adaptively weighted low-resolution images and simultaneous estimation of the regularization parameter," in *IEEE Int. Conf. Acoustics, Speech, Signal Processing*, vol. 3, May 2004, pp. 213–216.

[25] M. G. Kang and A. K. Katsaggelos, "Simultaneous multichannel image restoration and estimation of the regularization parameters," *IEEE Trans. Image Process.*, vol. 6, no. 5, pp. 774–778, May 1997.

[26] ——, "General choice of the regularization functional in regularized image restoration," *IEEE Trans. Image Process.*, vol. 4, no. 5, pp. 594–602, May 1995.

Authorized licensed use limited to: University of Ioannina. Downloaded on November 19, 2009 at 08:29 from IEEE Xplore. Restrictions apply.

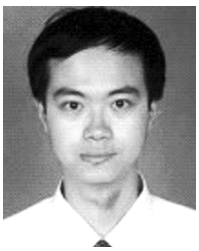

Hu He received the M.S. and Ph.D. degrees from the Department of Electrical Engineering, University of Buffalo, State University of New York, Buffalo, in 2002 and 2005, respectively.

His research interests include digital image processing and video communications, with s focus on super-resolution and restoration.

Lisimachos P. Kondi (M'99) received the Diploma degree in electrical engineering from the Aristotle University of Thessaloniki, Thessaloniki, Greece, in 1994, and the M.S. and Ph.D. degrees in electrical and computer engineering from Northwestern University, Evanston, IL, in 1996 and 1999, respectively.

During the 1999 to 2000 academic year, he was a Postdoctoral Research Associate at Northwestern University. Since August 2000, he has been an Assistant Professor of electrical engineering at the University of Buffalo, The State University of New York, Buffalo. During the summer of 2001, he was a U.S. Navy/ASEE Summer Faculty Fellow at the U.S. Naval Research Laboratory, Washington, DC. He is a Guest Editor of a special issue on video communications for 4G wireless systems to appear in the Wiley *Journal on Wireless Communications and Mobile Computing*. His current research interests include image and video processing and compression, wireless communications and wireless video transmission, image restoration and super-resolution, and shape coding.

Authorized licensed use limited to: University of Ioannina. Downloaded on November 19, 2009 at 08:29 from IEEE Xplore. Restrictions apply.